Catena 147 (2016) 258–268

Contents lists available at ScienceDirect

Catena

journal homepage: www.elsevier.com/locate/catena

Hyper-concentrated flow response to aeolian and fluvial interactions from a desert watershed upstream of the Yellow River

Zhijun Wang [a,b,c,*], Wanquan Ta [a]

[a] Cold and Arid Regions Environmental and Engineering Institute, Key Laboratory of Desert and Desertification, Chinese Academy of Sciences, 260 Donggang West Road, Lanzhou, Gansu Province, China
[b] School of Energy and Power Engineering, Lanzhou University of Technology, 287 Langongping Road, Lanzhou, Gansu Province, China
[c] University of Chinese Academy of Sciences, 19 Yuquan Road, Beijing, China

ARTICLE INFO

Article history:
Received 9 December 2015
Received in revised form 29 June 2016
Accepted 20 July 2016
Available online xxxx

Keywords:
Aeolian and fluvial interactions
Aeolian process
Arid zone
Desert watershed
Hyper-concentrated flow

ABSTRACT

Aeolian and fluvial interactions (AFIs) are critical earth-surface processes in arid zones, especially in desert watersheds. The response of hyper-concentrated flows to seasonal alternate AFIs shows very high rates of sediment transport and has important environmental and ecological consequences from local to global scales. Here, we present the aeolian processes-induced hyper-concentrated (AHC) flows that occurred in the Sudalaer desert watershed upstream of the Yellow River, which primarily transport non-cohesive coarse aeolian sand (>0.08 mm) and show a peak suspended sediment concentration (SSC) of 1.1 to 1.4 × 10^6 mg l^{-3}. Our field study and theoretical analysis indicate that non-cohesive coarse aeolian sand downstream in the channel can be entrained from the bed and can be suspended in the turbulent flow by the significant runoff generated upstream with a SSC γ_0 value of 0.5 × 10^6 mg l^{-3}. Severe aeolian processes can provide an abundant coarse sediment supply in the channel, which, once entrained, can also trigger and promote the development of AHC flows. We define, for the first time, the ratio of the weight percentage of coarse sediment to fine sediment $C_{>0.08\ mm}/C_{<0.05\ mm}$ as the optimal grain size indicator (OGI) in suspended sediment, indicating that, as the fraction of coarse sediment increases, the significant runoff gradually changes to hyper-concentrated flows and reaches the peak SSC when OGI = 3.25. Due to the high frequency of sandstorms and the infrequency of rainstorms, most of the significant rainfall-induced runoff with a certain SSC γ_0 can develop into AHC flows and can substantially contribute to the total sediment yield, even leading to deleterious effects on the downstream river system and ecology. Compared with other desert watersheds in semiarid regions, we propose that a SSC γ_0 of 500 kg m^{-3} is the threshold criteria for the occurrence of AHC flows in the arid desert watersheds. Comprehensive governing of soil erosion in the upstream gully-dissected slopes is an essential and effective measure for controlling AHC flows.

1. Introduction

Aeolian and fluvial interactions are basic geomorphic processes that control sediment transport and yield while shaping the landscape in arid zones (Breshears et al., 2003; Bullard and Livingstone, 2002; Bullard and McTainsh, 2003; Field et al., 2009; Langford, 1989; Tooth, 2000). Evidence has demonstrated that many active aeolian dunes terminate at stream channels and deliver a large volume of aeolian sand into the channels (Bullard and McTainsh, 2003; Nanson et al., 1995; Smith and Smith, 1984; Ta et al., 2008; Thomas et al., 1997). These abrupt additions of non-cohesive sand to stream channels can lead to narrowing, aggrading and damming of the heavily aeolian sand-filled channels (Anderson and Anderson, 1990; Jones and Blakey, 1997; Marker, 1977; Mason et al., 1997; Teller and Lancaster, 1986), resulting in an incredible 40-fold increase in bed load (Smith and Smith, 1984) and high suspended sediment loads during channel flooding. Although the extent of aeolian sand transport has been recognised, aeolian and fluvial erosion have historically been studied separately. Furthermore, the lack of simultaneous observations and field data limit the direct quantitative understanding of aeolian and fluvial interactions. Ta et al. (2014) proposed, for the first time, the effect of the aeolian process and its contribution to hyper-concentrated flows both theoretically and physically. The three fundamental driving factors (i.e., the channel bed slope, the aeolian-fluvial climate factor and the aeolian-fluvial geomorphological factor) causing hyper-concentrated flows, as suggested by Ta et al. (2014) are of great importance for regulating the ecological stability of desert watersheds.

Abbreviations: AHC, aeolian processes-induced hyper-concentrated; AFI, aeolian and fluvial interactions; SDC, Sudalaer desert channel; C>0.08 mm/C<0.05 mm, the ratio of weight percentage of coarse sediment to fine sediment; OGI, optimal grain size indicator; SSC, suspended sediment concentration.

* Corresponding author at: Cold and Arid Regions Environmental and Engineering Institute, Key Laboratory of Desert and Desertification, Chinese Academy of Sciences, 260 Donggang West Road, Lanzhou, Gansu Province, China.
E-mail address: wzj1159@163.com (Z. Wang).

http://dx.doi.org/10.1016/j.catena.2016.07.033
0341-8162/

To understand these complicated processes in depth, we studied the Sudalaer desert watershed in the upstream area of the Yellow River in China, which is a typical watershed characterised by aeolian and fluvial interactions (AFIs). Our main objective is to further explain the mechanism and characteristics of aeolian processes-induced hyper-concentrated (AHC) flows based on the field observation of four flood events from August 2011 to July 2012 (23 August 2011, 18 July 2012, 19 July 2012 and 27 July 2012) that occurred in the study area to provide additional criteria for predicting AHC flow occurrence and to provide advice on controlling measures in arid and semiarid watersheds.

2. Study area

The Sudalaer desert watershed is an ephemeral desert channel located on the southern margin of the Hobq Desert in the Ordos plateau of China (Fig. 1b and c) and is one tributary of the Maobulang desert channel (Fig. 1b, T1). Composed of 32-km^2 gully-dissected slopes and 21-km^2 dune-covered slopes, the Sudalaer desert watershed has an area of approximately 59 km^2, with an 8-km-long aeolian sand-filled channel extending northeast by north that deviates approximately 38° with respect to the north direction, whose average channel slope is 0.0058. The gully-dissected slopes, distributed on the southeastern part of the upstream reach of the Sudalaer desert channel (SDC), are characterised by severe fluvial erosion and are the primary runoff-generating areas in the watershed, with widespread exposure of subsurface Cretaceous sandstone rocks. A low thickness of aeolian sand sheets covers parts of these gully-dissected slopes because of weak aeolian erosion. However, in the northwestern part of the downstream reach of the SDC, active sand dunes migrate southeasterly, which are dominated by aeolian processes, and terminate at the SDC. During the windy winter and spring seasons (December to May), large volumes of aeolian sand are delivered into the SDC, while in the rainy summer season, these aeolian sand deposits may be flushed downstream by rainfall-induced floods, consequently contributing to AHC flows.

As shown in Fig. 2, the left margin of the SDC is always covered with 2 to 10-m-high, active transverse aeolian dunes that migrate toward the downwind direction to the channel under the influence of W-, NW- and NNW- winds and deliver a large volume of aeolian sand into the channel. Occasionally, some channel sections are fully blocked by sand dunes during the windy seasons. This continuous and abundant sand input may constitute the significant contribution to the total fluvial sediment yield under certain hydraulic conditions. According to historical flooding records monitored by the Tugerige gauge station in the Maobulang desert channel from 1981 to 2010, rainfall-induced floods (>500 m^3 s^{-1}) occurred once every 3 or 4 years (Ta et al., 2015). This suggests that as the tributary of the Maobulang desert channel, the SDC is likely to experience heavy rainfall with the same frequency. Thus, the sediment-laden floods (i.e., runoff) generated from the upstream rills or gullies always develop into AHC flows downstream by entraining aeolian sand sediment available in the channel. Some of these AHC flows merge into the Maobulang desert channel and deliver large volumes of sediment into the Yellow River, leading to the formation of cross-channel sand dams and resulting in catastrophic floods (Zhi and Shi, 2002).

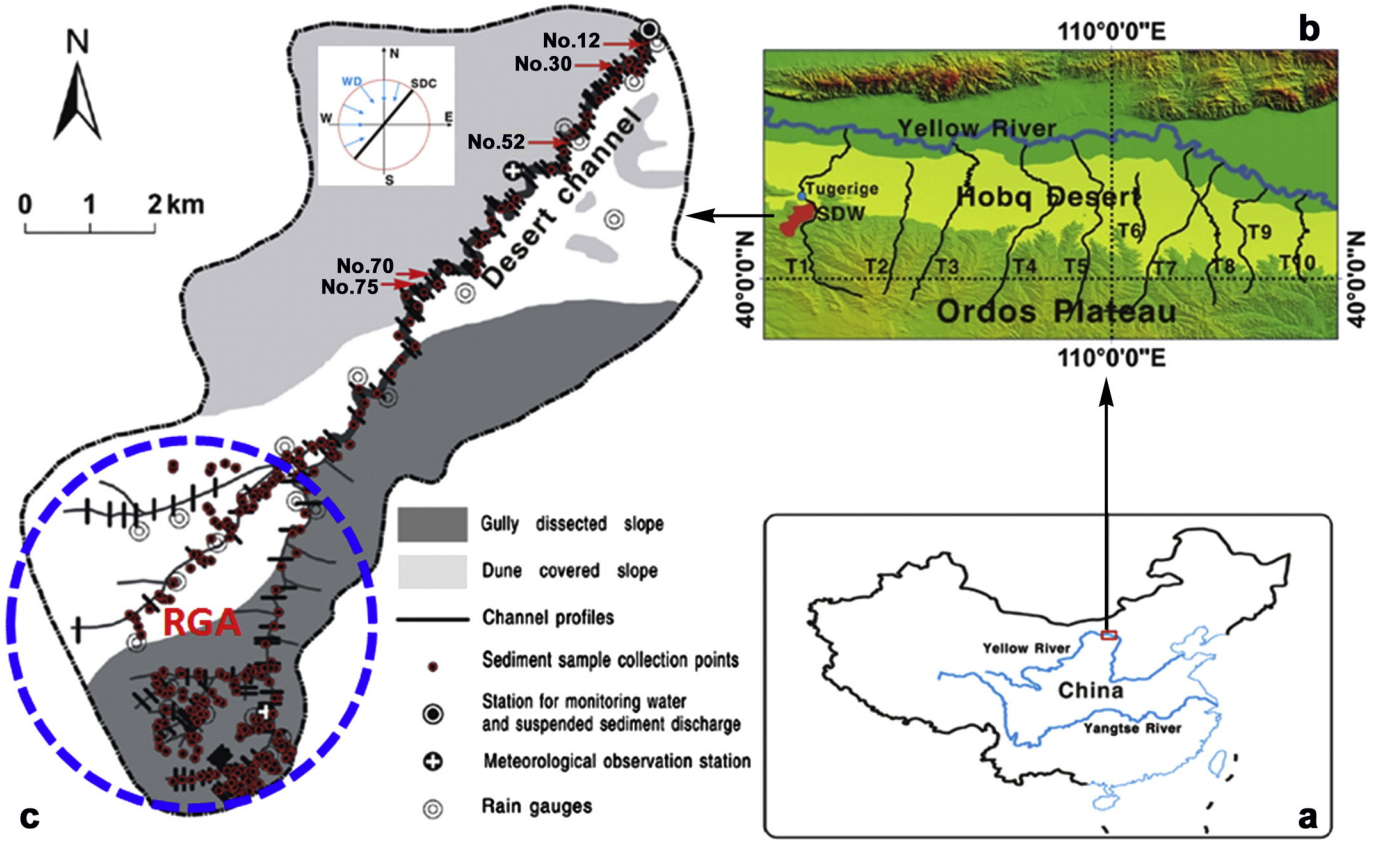

Fig. 1. Location of the Sudalaer desert watershed and the distribution of the sand-dune slopes, gully-dissected slopes and the desert channel: (a, b) Location of the Sudalaer desert watershed showing the juxtaposition of the Hobq Desert. T1–T10 are the ten ephemeral cross-desert tributaries flowing from south to north into the Yellow River. T1 denotes the Maobulang ephemeral desert channel to which the Sudalaer desert channel is a tributary. Tugerige is a gauge station. SDW is the Sudalaer desert watershed; (c) Plan view of the Sudalaer desert watershed showing asymmetrically distributed sand dunes and gully-dissected slopes, between which the white region is a transitional loess zone characterised by weak aeolian-fluvial erosion, of which 10–30% is covered with *Artemisia ordosica* Krasch shrubs, and the blue dashed circle shows the runoff-generating area (RGA). No. 12, No. 30 and No. 52 are examples of the surveyed profiles shown in Fig. 11, and No. 70 and No. 75 are the two profiles chosen for air flow measurement, as shown in Fig. 4. WD is the wind direction from which aeolian sand can be transported into the SDC. (For interpretation of the references to colour in this figure legend, the reader is referred to the web version of this article.)

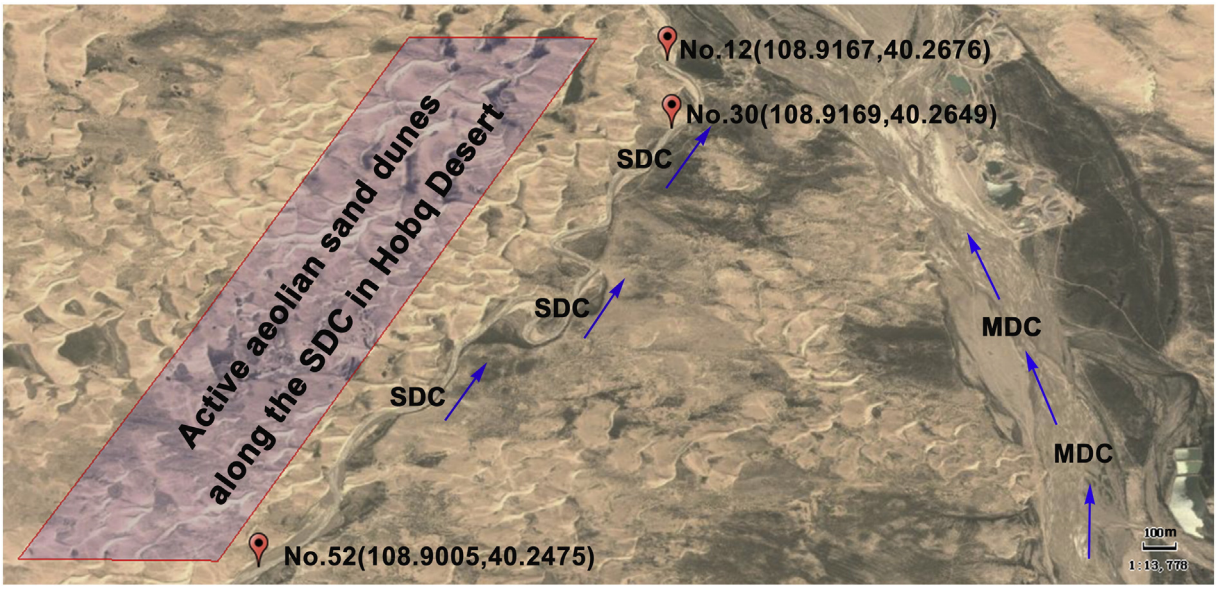

Fig. 2. Aerial photograph of the SDC and the location of the representative cross-sections. MDC is the Maobulang desert channel. The values in the brackets show the longitude and latitude of the representative cross-sections.

In summary, the SDC is susceptible to seasonal alternate AFIs and shows seasonally variable geomorphic characteristics. Therefore, we chose it as an ideal location to investigate AFIs and their related AHC flows.

3. Methods

3.1. Observation of aeolian process-induced channel filling

The Hobq Desert has long been our observation field for aeolian processes, and basic data have been collected about the wind and aeolian sand. The number of annual strong wind days is 10–32 d on average, and the number of annual sandstorm days is 19–22 d, showing a high frequency of occurrence, especially in spring. The annual mean wind speed value is 3.7 m s^{-1}. For the active sand dune areas in the Hobq Desert, continuous field studies dominated by the Cold and Arid Regions Environmental and Engineering Institute, Chinese Academy of Sciences have established the empirical relationship between the unit sand transport rate q_{sw} (g cm^{-1} min^{-1}) and the critical entrainment wind speed V (m s^{-1}) as follows:

$$q_{sw} = 0.088V^3 \quad (1)$$

According to Eq. (1) and because of the severe channel filling in the SDC, we propose that wind speed variation with respect to the terrain across the channel section plays an important role in sand transport and deposition. Therefore, two representative channel sections in the SDC are chosen to measure the air flow (wind speed at a height of 1 m with a measuring time interval of 5 s and with reference to the HOBO automatic meteorological observation instrument) of a wide cross-section and a narrow cross-section, respectively, using a CR 1000 anemometer on 5 October 2014, to determine the deposition of aeolian sands on the lee side of the channel.

Two HOBO automatic meteorological observation instruments were installed in the gully-dissected and dune-covered slopes, respectively, to monitor the change in wind speed and rainfall intensity in the watershed, thus estimating the aeolian process-induced channel filling and the ratio of sandstorm frequency to rainstorm frequency.

The amount of channel filling was estimated following Jackson and Hunt (1975) as follows:

$$Q_T = \sum_{i=1}^{n} q_i t_i l_i \sin\theta_i \quad (2)$$

where Q_T is the annual deposition of aeolian sands in the channel, q_i is the unit sand transport rate per hour with respect to the average wind speed v_i, t_i is the duration of the wind speed greater than the critical entrainment wind speed, l_i is the channel length under the influence of the corresponding wind direction, and θ is defined as the anticlockwise angle from the wind direction to the channel section ($0° < \theta < 180°$).

3.2. Observation of fluvial process-induced channel scour

One hundred and eighty channel cross-sections were installed at the end of the windy season in May 2011, of which eighty cross-sections were installed in the SDC at average intervals of 80 m, and the remaining cross-sections were installed in channels in the upstream basin. Each cross-section was marked out using two temporary benchmarks and surveyed using an FTS832 total station (Tianjin Optical Precision Instrument Co., Ltd., China). The prism distance measurement mode was used with an accuracy of ±(2 mm + 2 ppm). These cross-sections were re-surveyed at the end of the windy season in May 2012 and after the four flood events during our study period to estimate the scour and fill sediment volume per unit channel length (unit: m^3 m^{-1}). As the left channel margin in the desert stretch is covered with aeolian dunes, the volume of eroded aeolian dunes may be considered as the contribution to the total fluvial sediment yield. We chose a relatively straight channel section at the exit of the SDC with a fine-gravel bed at the outlet of the watershed to make a fixed, trapezoid-shaped concrete cross-section, over which a single float-type water level meter was set in 2011 (Fig. 3a). In 2012, an ultra-sonic level meter was used instead to automatically monitor the flood water levels (Fig. 3b). Discharge measurements were obtained primarily during flood events by measuring the water level and converting the water level to discharge using the method provided by Ta et al. (2015). During the flood events, suspended sediment samples within 50 cm of the water surface were taken using a 480-ml and 550-ml bottle fixed to a 2.5-m-long stainless steel rod. The interval between samples was 1–2 min during the rising limb of the hydrograph and the peak, whereas

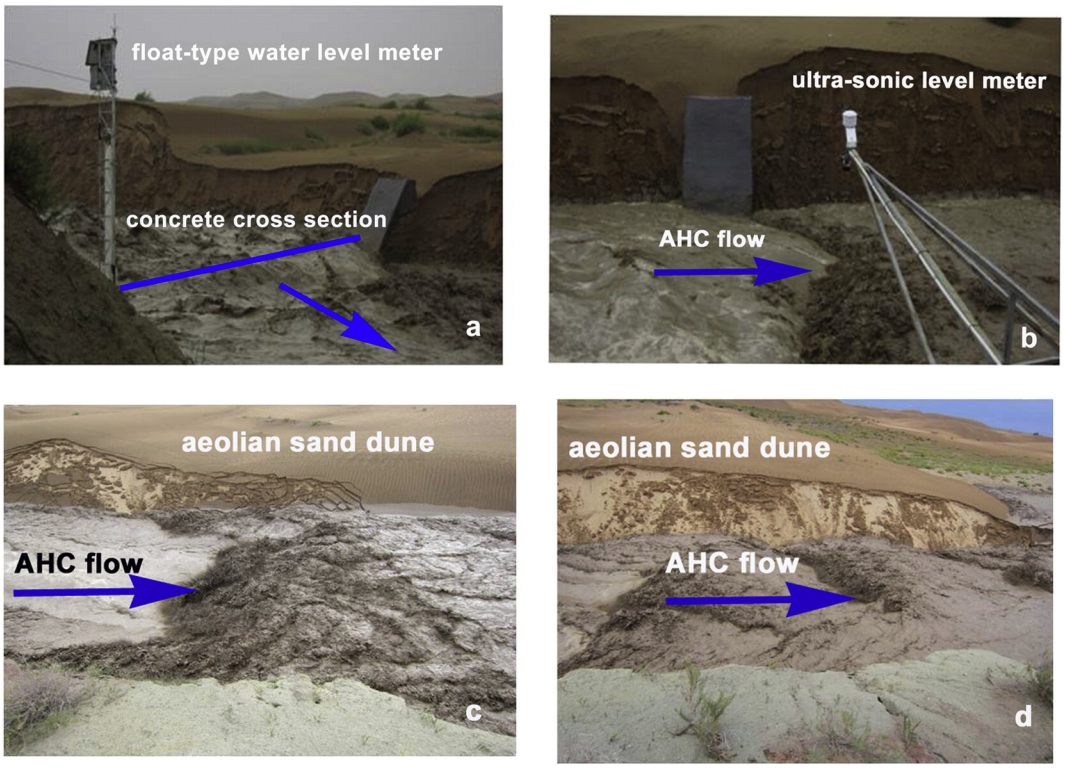

Fig. 3. Photographs of the measuring method of AHC flows (a), (b) and the development of AHC flows on 23 August 2011. (c) The flow initially flushed through the SDC; (d) The flow eroded the sand dune on the left bank. The arrows show the flow direction.

it was 3–10 min during the recession limb. The dry weight of the samples was used to determine the suspended sediment concentration and was sieved to determine the size distribution of the suspended sediments. We also installed rain gauges (18 gauges in 2011 and 28 gauges in 2012) in the Sudalaer watershed to monitor the spatial and temporal distribution of rainfall and to evaluate the disparities between the slope erosion of the gully-dissected and dune-covered slopes. To investigate the surface material composition in the study area and to provide supportive evidence that the aeolian process was contributing to the fluvial sediment yield, we also collected 200 hillslope surface sediment samples and 34 samples from the aeolian dunes within 20 cm of the surface along the desert channel at an average interval of 200 m. The grain size was measured as compared with that of the suspended sediment samples.

All of these measurements can provide adequate data to determine the effect of AFIs on the study area.

4. Results

4.1. Aeolian processes and the related channel filling

The SDC extends northeast by north and deviates approximately 38° with respect to the north; however, the prevailing winds in the study area are W-, NW- and NNW-; thus, the SDC section is approximately 45° to 130° for the main wind directions. The annual mean critical entrainment wind speed value in the study area is 4.9 m s^{-1}, and the monthly mean value is 3.6 m s^{-1}. Our air-flow measurements indicate that wind speed varies with the terrain and reaches the maximum on the top of the sand dune, while at the bottom, it drops to the minimum. As shown in Fig. 4a and b, the relative wind speed value was 1.18 and 1.05 on the top and decreased to 0.2 and 0.88 at the bottom for the wide and narrow cross-sections, respectively. During this period, most of the coarse aeolian sands carried by wind are most likely to be separated and deposited on the lee side of the channel, regardless of whether the wind direction is normal for the local channel section. When the wind direction is normal to the channel section, the partial vector of air flow obstruction is greater (Jackson and Hunt, 1975), which ultimately facilitates the coarse aeolian sands deposition, and wind-blown sands are delivered to the channel directly. Then, the wind speed accelerates gradually to the maximum on top of the gully (1.35 for the wide cross-section and 1.42 for the narrow cross-section). In this process, the air flow carrying aeolian sands blows through the channel bottom to the gully slopes and is blocked to deposition, consequently completing the channel filling process. The SDC is a fine gravel-bed channel, but in the desert stretch, the gravel bed is always covered with 10 to 60-cm-thick aeolian sand during the windy seasons; occasionally, some channel sections are also fully blocked by sand dunes.

Corresponding to the dominant wind direction in the study area, the maximum value of the unit sand transport rate occurred at the W- direction, and the sand transport rate from November to April is approximately equal to the annual sand transport rate (Fig. 5). In addition, as shown in Fig. 6, the period of the high sand transport rate value occurs in winter and spring in the Hobq Desert (maximum in April and the second maximum in November), of which the spring season contributed most of the aeolian sand input. Here, we estimated the aeolian sand channel filling in 2011 from Eqs. (1) and (2) according to the measured data of the duration of 16 wind directions and the modeled unit sand transport rate of the SDC in the spring of 2011 (Fig. 7) to approximately represent the annual situation, and using the same method, the values of 2012 and 2013 were obtained (Table 1).

4.2. Earth surface material composition and significant runoff generation

Our field observation indicated that there was runoff in the upstream hills or gullies in the Sudalaer desert watershed but not in the downstream dune-covered slopes. In other words, the dune-covered slopes did not generate significant runoff that leads to AHC flows in response to heavy rainfall compared with the gully-dissected slopes. Intensive erosion effects on the earth surface material composition are proven to be the significant reason for the formation of AHC flows.

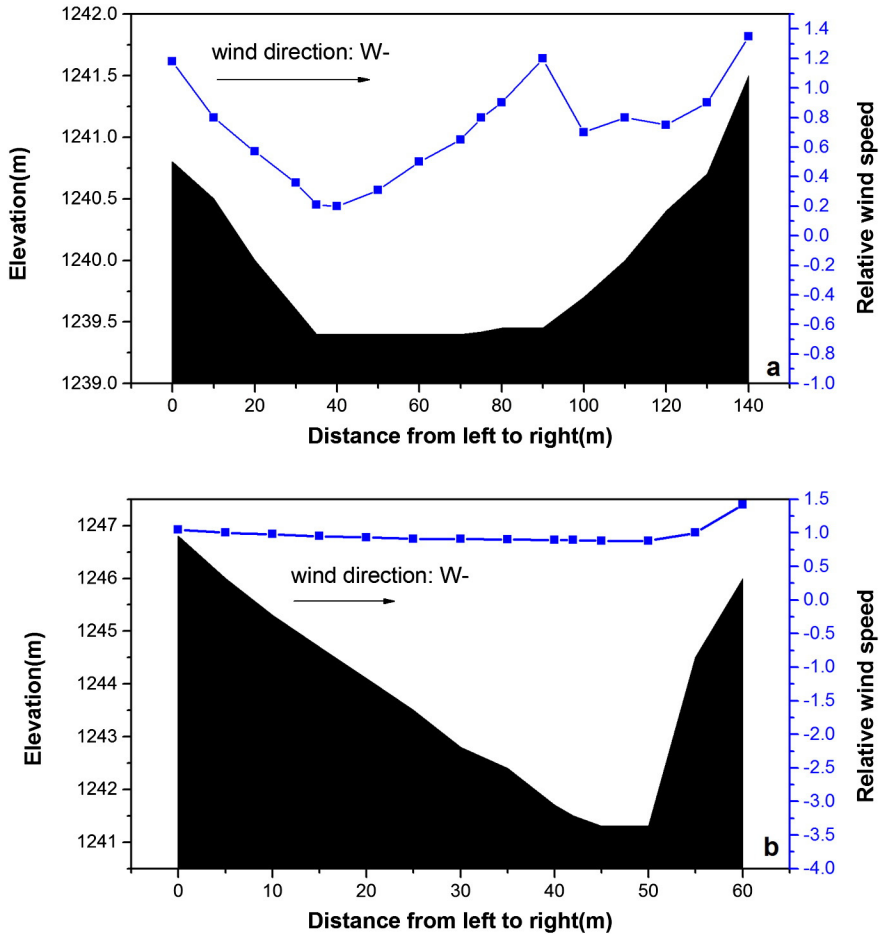

Fig. 4. Cross-section air flow over a wide cross-section (a); and a narrow cross-section (b). Note that the meteorological observation station in the desert channel as shown in Fig. 1c is chosen as the reference site, and all of the measured wind speed values (at a height of 1 m) were converted, with the measuring time interval as 5 s, to relative wind speed, i.e., the ratio of the measured wind speed value in the channel to that in the reference site (Jackson and Hunt, 1975) within 5 min.

The upstream area of the SDC is characterised by gullies and rills caused by severe fluvial erosion. Infrequent but heavy rainstorms, sparse vegetation cover and highly erodible Cretaceous sandstone rock exposure (Fig. 8) are regarded as the fundamental natural factors responsible for the formation of AHC flows. In the downstream desert stretch, intensive aeolian erosion provides an abundant aeolian sand supply, which was sampled and measured to be coarse particles (>0.08 mm). The fraction of these coarse components reaches nearly 90% (Table 2). These aeolian sands may be transported by floods as part of the coarse sediment supply. In other words, these earth surface material conditions in the desert channel of the SDC are considered as the essential natural factor to the development of AHC flows. Our field investigation also showed that the surface (20-cm thickness) of the gully-dissected slopes is loose and highly erodible Cretaceous sandstone

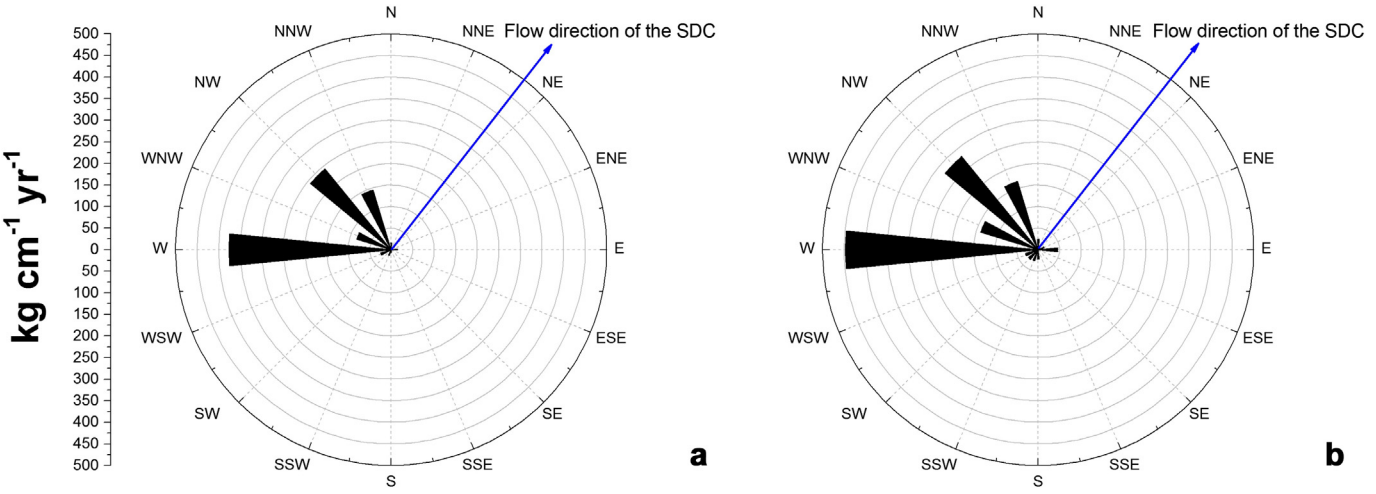

Fig. 5. Distribution of the modeled unit sand transport rate in sixteen wind directions of the active sand dunes area in the Hobq Desert: (a) Unit sand transport rate from November to April; (b) Annual unit sand transport rate.

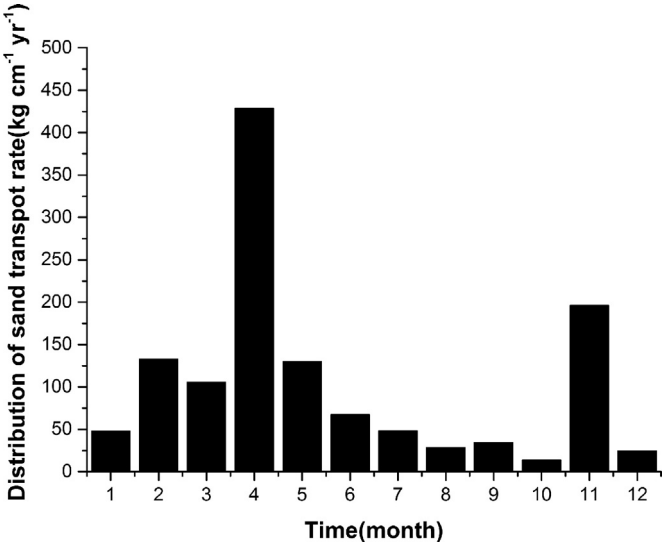

Fig. 6. Distribution of monthly unit sand transport rate of the active sand dunes area in the Hobq Desert. Note that the unit sand transport rate is modeled using Eq. (1).

rocks thickly covered by aeolian sand, with half of their particle components being median and coarse (Table 2; >0.05 mm). Even excluding the components of coarse aeolian sand sheets, the pure Cretaceous sandstone rock should still be considered coarser. Nevertheless, these sandstone rocks are apt to be softened while absorbing water and will scatter rapidly to become particles with sizes <0.05 mm and even <0.01 mm to form a uniform water-sediment mixture when a heavy rain or rainstorm arrives. This is similar to the formation of the rainfall-induced runoff (Xu, 2005a, 2005b) in the 40 representative tributaries of the middle reach of the Yellow River, of which the particles mixed with water as uniform suspended sediment are fine particles (<0.01 mm) originating from the loess material widespread there. As the runoff mentioned above (uniform water-sediment mixture) plays a critical role in forming and developing AHC flows, similar to those in the loess plateau of the Middle reach of the Yellow River, here, we define sediment <0.05 mm in diameter as the fine sediment supply generated in the upstream rainfall-induced runoff. Both the fine sediment and the coarse sediment can exist in the AHC flow in the form of suspended sediment under certain conditions.

AHC flow is a type of two-phase flow composed of a solid phase and a liquid phase, of which the aeolian sands filled in the channels contribute large volumes of non-cohesive solid-phase components to the SDC. Entrainment of these aeolian sands by clear water is not easily accomplished, even by flood turbulence, without a certain proportion of fine particles. In general, heavy rainfall occurring in the upstream gullies or rills in the Sudalaer watershed mixes rapidly with fine particles and creates a dense and uniform particulate flow, i.e., the liquid phase with the suspended sediment concentration (SSC) γ_0 that travels downstream. This process increases and maintains the SSC and the suspension, maintains the flow of the water-sediment mixture against the bed shear stress, and develops as significant runoff with a powerful impelling force, leading to erosive AHC flows by entraining the supplement supply of coarse aeolian sand as suspended sediment.

4.3. Fluvial process and AHC flow-induced channel scour

As the rainfall-induced runoff with a certain SSC γ_0 value flushed downstream along the SDC, the flood ultimately developed into an AHC flow with a maximum SSC γ because of the supplement of the aeolian sands stored in the channel (Fig. 3c and d). The floods in the SDC had an extremely high peak SSC of 1.1–1.4 × 10^6 mg l^{-3} and showed a rapid rise and fall in flow discharge in response to 35–60 mm rainstorms with a rain intensity >0.27 mm min^{-1} (Fig. 9).

As shown in Fig. 9, the peak SSC met approximately well with the peak discharge and demonstrated an obvious phenomenon of low runoff with high SSC levels, which was mainly attributed to the short flood travelling time from the upstream runoff-generating area to the downstream aeolian sediment source area and the increase in the impelling force of the runoff due to the coarse aeolian sands supplement in the SDC. Although the SSC increased rapidly with respect to the flooding, the recession was slower, showing an obvious anti-clockwise hysteresis (Klein, 1984; Ta et al., 2015) between the flow discharge and the SSC. This result suggests that the sediment transport ability of the floods was subject to sediment availability in the aeolian sand-filled channel.

Our sampling analysis indicated that the crucial component of the suspended sediment was 0.08–0.2 mm in these four floods and that the SSC in these AHC flows increased with the increasing 0.08–0.2 mm fraction of the aeolian sands. Moreover, it appeared to be an optimal proportion between fine and coarse sediment that led to the maximum SSC of AHC flows, as shown in Fig. 10. Here, we define the ratio of the weight percentage of the coarse particles ($C_{>0.08\ mm}$) to that of the fine particles ($C_{<0.05\ mm}$) as the optimal grain size indicator (OGI, $C_{>0.08\ mm}/C_{<0.05\ mm}$), and the result indicated that if OGI = 3.25, then the SSC increases to the maximum of 1.18 × 10^6 mg l^{-3} (approximately the average value of 1.1–1.4 × 10^6 mg l^{-3}). If OGI = 1, then the value of SSC is close to 0.65 × 10^6 mg l^{-3}, which further verified that "the coarse sediment content was greater than 50% when the SSC was higher than 0.5 × 10^6 mg l^{-3}" and that the aeolian processes were contributing to the fluvial sediment yield (Ta et al., 2015). In addition, when the SSC decreased to 0.5 × 10^6 mg l^{-3}, the related OGI dropped to below 0.65, which indicated that most of the sediment contents were composed of fine particles from upstream gully-dissected slopes, resulting in the disappearance of the AHC flow or revealing that the AHC flow should not occur. Therefore, we suggest that γ_0 = 0.5 × 10^6 mg l^{-3} is the SSC threshold of the significant run-off leading to AHC flows in the SDC (Fig. 10).

Stream channel erosion has long been suspected as the major contributor to long-term sediment yield from the Sudalaer watershed, and its contribution to hyper-concentrated flows has not been reported until recently (Ta et al., 2015). Our channel survey and resurvey studies with field observations and calculations, combined with the aerial digital data of the cross-sections before and after the four flood events, indicated high fluvial scour rates of aeolian sand deposits during the passage of the four floods but low aeolian sand fill rates during the aeolian processes. The annual channel erosion attributed to the fluvial erosion of the SDC shown in Table 3 compared with the annual channel fill in Table 2 indicated that the ratio of the annual channel scour rate to the channel fill rate was approximately 3:1 and 4:1 from 2011 to 2012. It seems that aeolian processes may not provide an abundant coarse sediment supply. However, the rainstorm frequency is once every three to four years. This natural phenomenon of infrequent rainfall rate and frequent sandstorm rate enables adequate coarse aeolian sands to be filled in the channel in the spring and scoured by rainfall-induced floods with a certain content of fine particles in the rainy season. This result was also supported by the flow discharge data from the Tugerige gauge station in the MDC (Fig. 1b) that a high sediment load flood (>500 m^3 s^{-1}) occurred once every three to four years on average from 1981 to 2010 (Ta et al., 2015).

Our field observation and measurement of the channel section profiles also demonstrated that both the left margin and the bottom of the SDC were severely flushed (Fig. 11), because the left margin was covered with aeolian dunes and the bottom was filled with aeolian sands. Particularly, the surveyed channel profile No. 30 (Fig. 11b) represents a channel section full of aeolian sands before the flood in August 23, 2011, which ultimately was flushed to show a narrow channel profile after the flood on July 27, 2012, and this implied that a nearly 2-m-thickness of aeolian sands migrated into the channel by severe aeolian processes over a one-year period. Although these floods eroded large quantities of aeolian sand from the SDC, its left margin was still covered

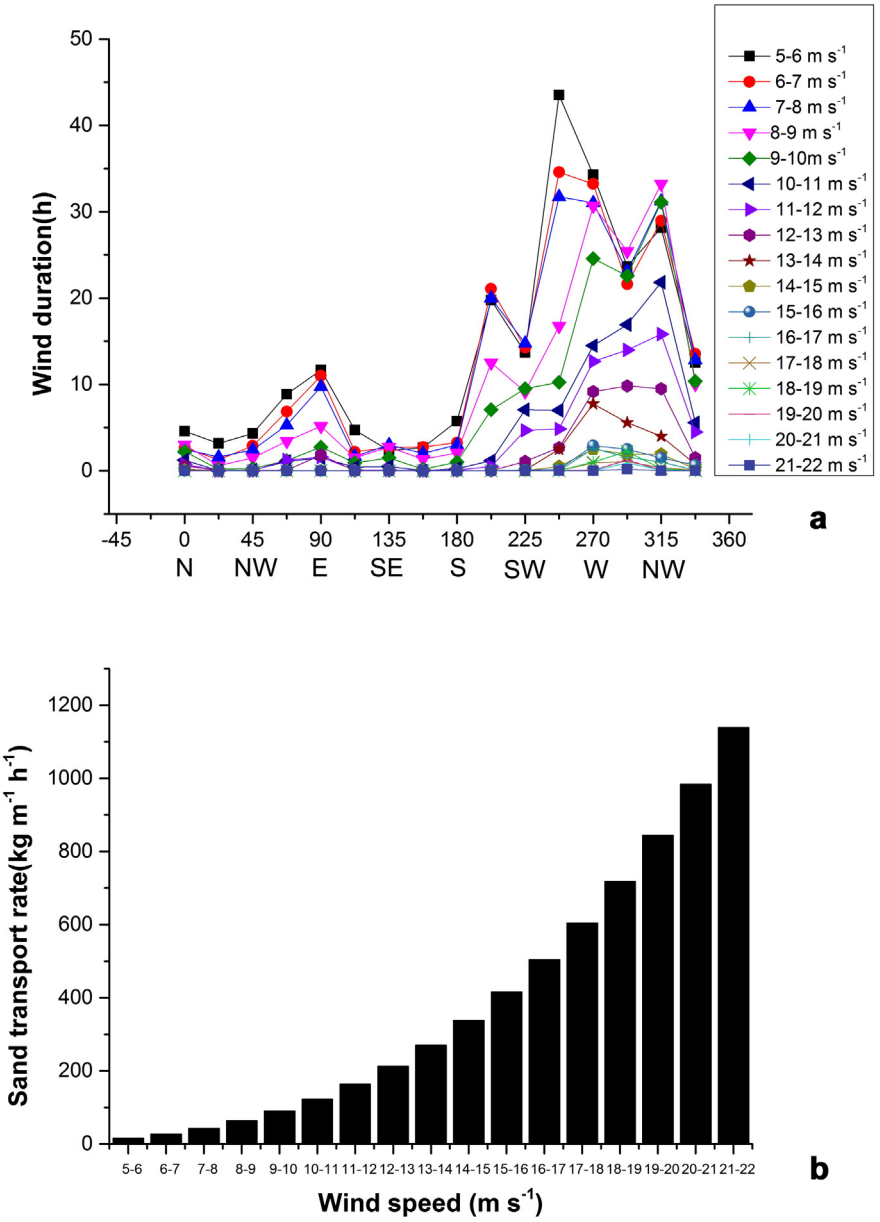

Fig. 7. Duration of critical entrainment wind speed in sixteen directions in the SDC in the spring of 2011 (a) and the wind speed-related sand transport rate modeled using Eq. (1) (b).

by aeolian dunes. This suggests that the SDC still has an adequate store of aeolian sands, which is likely to contribute to the fluvial sediment yield during subsequent flooding.

5. Discussion

Our results indicate that seasonal alternate aeolian and fluvial interactions play an essential role in causing hyper-concentrated flows in the SDC. Although intensive aeolian activities in winter and spring seasons are powerful sediment transport processes, they cannot carry coarse aeolian sand across the desert channel, thus leading to the temporary accumulation of aeolian sand in the channel bed. This coarse aeolian sand supply, when the infrequent but heavy summer rainfall generated from the upstream gullies arrives, contributes enough transportable sediment to the runoff and leads to AHC flow in the desert channel and even promotes the development of AHC flow. Many previous studies argued that aeolian and fluvial processes need to be studied separately because dune-covered areas have high infiltration rates, therefore having reduced runoff and fluvial processes (Tsoar, 1990). In addition, runoff-generating areas have relatively high vegetation cover that suppresses aeolian processes (Buckley, 1987; Lancaster and Baas, 1998; Wasson and Nanninga, 1986; Wolfe and Nickling, 1993); this has led to long-term separation of the study of aeolian and fluvial processes not only in arid and humid zones but also in small desert watersheds. Although in recent years, an increasing number of studies has focused on the interactions between river and desert systems (Belnap et al., 2011; Draut, 2012; Liu and Coulthard, 2014; Sankey and Draut, 2014), field works and even the mechanisms about the effect of aeolian processes on the related hyper-concentrated flows have not yet been discussed comprehensively until now.

In theory, when a sandstorm blows across a stream channel at angle θ, a recirculating air flow immediately develops in the opposite direction

Table 1
Annual channel fill in the SDC from 2011 to 2013.

Time (yr)	2011	2012	2013
Channel fill (10^4 t)	8.34	8.66	6.83

Fig. 8. Photograph of the upstream gully-dissected slopes composed of erodible Cretaceous sandstone rocks.

in the channel. As a result, the wind speed measured at the channel experienced a decrease on the lee side of the channel slope and an increase on the slope of the other bank. The recirculating air flow leads to separation and deposition of coarse aeolian sands on the lee side of the channel slope. In general, the aeolian sand transport rate is dependent on wind speed and grain size and can be described as follows (Bagnold, 1941):

$$q_{sw} = C_1\sqrt{\frac{d}{D}}\frac{\rho_a}{g}U_*^3 \tag{3}$$

where q_{sw} is the aeolian sand transport rate, C_1 is an empirical dimensionless constant (1.8 for the naturally graded sands occurring in dunes), d is the diameter of a standard 0.25-mm sediment, g is the gravitational acceleration, U_* is the wind shear velocity during saltation, and ρ_a is the air density. Following Sauermann et al. (2001), the shear velocity in Eq. (3) can be expressed as follows:

$$U_* = \frac{v(z)\mathcal{K}}{\ln\frac{z}{z_0}} \tag{4}$$

where $v(z)$ is the wind velocity at a height z over the sand surface, $\mathcal{K}$ is the von Kaman constant (0.4), and z_0 is the roughness length of the sand surface. From Eqs. (3) and (4), the aeolian sand transport rate can be expressed as follows:

$$q_{sw} = \alpha v^3(z) \tag{5}$$

$$\alpha = C_1\sqrt{\frac{d}{D}}\frac{\rho_a K^3}{g\left(\ln\frac{z}{z_0}\right)^3} \tag{6}$$

Table 2
Earth surface material composition and grain size distribution in the Sudalaer watershed.

Sample name	Grain size fraction (%)			
	>0.2 mm	0.2–0.08 mm	0.08–0.05 mm	<0.05 mm
Aeolian sand	6.51	78.9	13.03	1.56
Cretaceous sandstone rocks	20	26	8	46

The empirical equation (Eq. (1)) we used based on continuous field observations of the active sand dunes in the Hobq desert is consistent with Eq. (5) in substance, and the critical entrainment wind speed v in Eq. (1) is equal to the wind velocity at a height of 10 m over the sand surface (i.e., the meteorological observation height) and $\alpha = 0.088$.

Our results indicate that both aeolian and fluvial processes that are well developed in a desert watershed are required for hyper-concentrated flows to occur, and there is an optimal ratio of different grain size sediment contents in the flows, indicating the severity of the effect of aeolian and fluvial erosion on different earth surface materials. Here, the proposed OGI ($C_{>0.08\ mm}/C_{<0.05\ mm}$) can well indicate that coarse sediment was eroded by aeolian processes downstream and the fine sediment merged uniformly with water by rainstorm-induced fluvial erosion upstream, consequently resulting in the occurrence, development and disappearance of AHC flows in the Sudalaer desert watershed.

When a rainstorm occurs in the AFI watershed, the dune-covered area cannot produce a runoff due to high infiltration; however, the runoff can be produced in the gully-dissected area to form a flood with a SSC γ_0. This significant runoff is critical for the formation of AHC flows, which can be explained in theory as follows. During the passage of the significant runoff with a SSC γ_0, a dense particulate flow forms, and the ability to maintain the flow against the bed shear stress improves. When the entrainment rate of the aeolian sands from the channel bed exceeds the sediment deposition rate, the flow will obtain more sediment from the bed than it will lose through deposition, leading to an increase in SSC and an increase in the impelling force per unit fluid mass due to gravity acting on the flow (Parker et al., 1986). The mechanism can also be clearly indicated by the mass, moment and energy balance equations for the AHC flows described by Onoe et al. (1985), Pantin (1979), Parker et al. (1986), and Winterwerp et al. (1992) as follows:

$$\frac{\partial\gamma h}{\partial t} + \frac{\partial u\gamma h}{\partial x} = \sigma(F_e - F_d) \tag{7a}$$

$$\frac{\partial Uh}{\partial t} + \frac{\partial U^2 h}{\partial x} = \frac{\sigma-\rho}{\sigma}g\gamma hS - v_*^2 \tag{7b}$$

$$\frac{\partial Kh}{\partial t} + \frac{\partial UKh}{\partial x} = v_*^2 U - \frac{\sigma-\rho}{\sigma}gv_s\gamma h - \frac{1}{2}(\sigma-\rho)ghv_s(F_e - F_d) \tag{7c}$$

where σ is the density of the aeolian sand particles, ρ is the density of water, γ is the sediment concentration in the AHC flow, h is the thickness of the flow, U is the mean transport velocity, F_e is the entrainment rate of the aeolian sands from the channel bed, F_d is the sediment deposition rate, g is the gravitational acceleration, S is the channel bed slope, and v_* is the flow shear velocity over the channel bed. If F_e exceeds F_d, then the flow accelerates, the bed stress and channel erosion increase, and more aeolian sand is entrained into the flow, thus developing the AHC flow.

This special AFI is not unique and was also observed in the Xiliugou desert channel across the Hobq Desert in the Ordos Plateau (T4, Fig. 1b), whose geomorphologic characteristics are similar to the Maobulang desert channel (T1) and the SDC. However, it is a transitional region from desert to loess, with an arid and semiarid climate. The upstream gully-dissected slopes are thinly covered by loess instead of aeolian sand because the downstream desert stretch is composed of widespread semi-fixed dunes rather than active dunes. Thus, the AHC flows at this location, show finer sediment of <0.01 mm in diameter and less coarse sediment of >0.08 mm in diameter in suspended sediment. Thus, the SSC threshold was proposed to be 300 kg m^{-3} with reference to the hyper-concentrated flows in the Middle reach of the Yellow River (Xu, 2013).

In the SDC, as shown in Fig. 10, when OGI is close to 1.0, the runoff begins to form dense particulate flow and obtains a greater ability to entrain more aeolian sands against the bed shear stress. The corresponding SSC is approximately 0.5×10^6 mg l^{-3}, while OGI exceeds 1.0; the

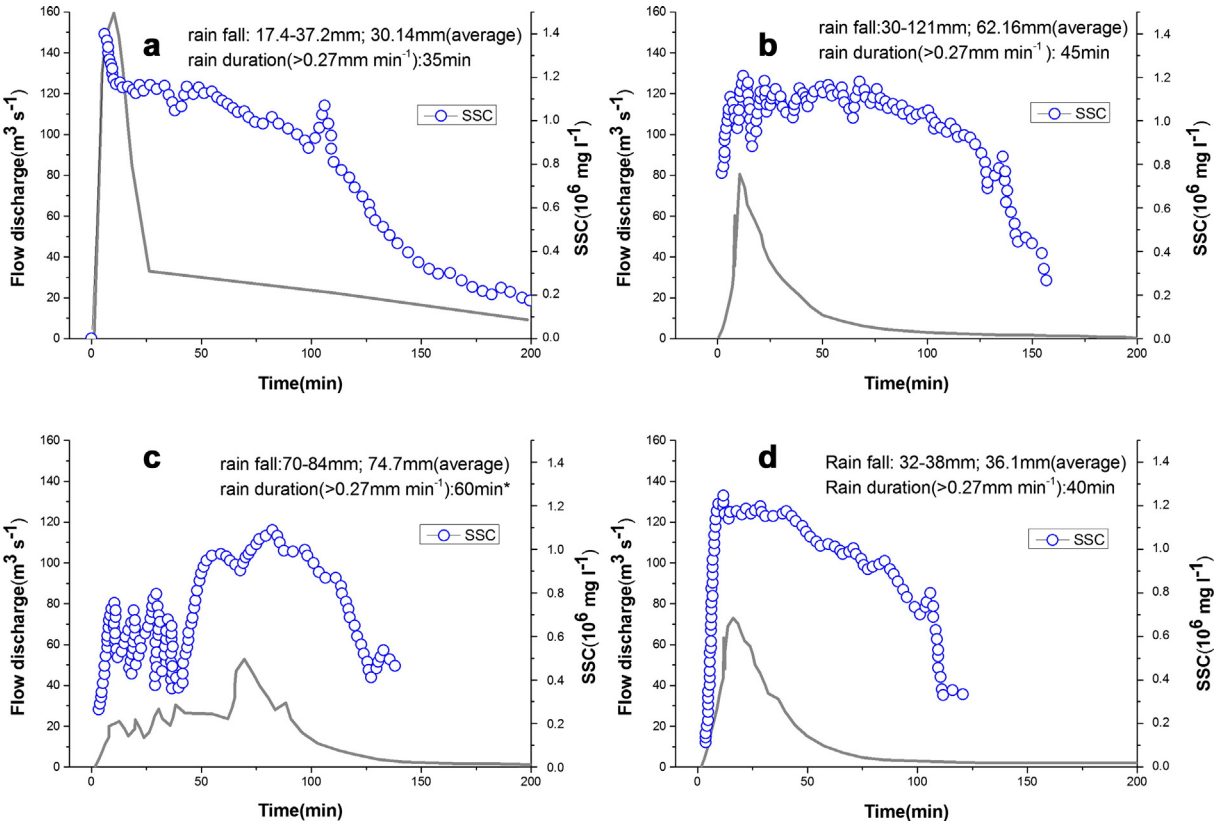

Fig. 9. Hydrographs and the related dynamic variation of the suspended sediment concentration (SSC) of the flood events: (a) 23 August 2011; (b) 18 July 2012; (c) 19 July 2012; (d) 27 July 2012.

suspended sediment components become coarse aeolian sand dominant, and AHC flows occur and develop to the peak SSC. We define 0.5×10^6 mg l^{-3} as the threshold SSC and, furthermore, suggest that the threshold SSC for the occurrence of AHC flows in arid desert watersheds in the upstream of the Yellow River should be 500 kg m^{-3}. Because AHC flows always show very high rates of sediment transport and lead to deleterious downstream effects on the river system and ecology, we propose that planting trees and grass to prevent the upstream gully-dissected slopes from severe soil erosion and related runoff generation is the effective measure to control AHC flows.

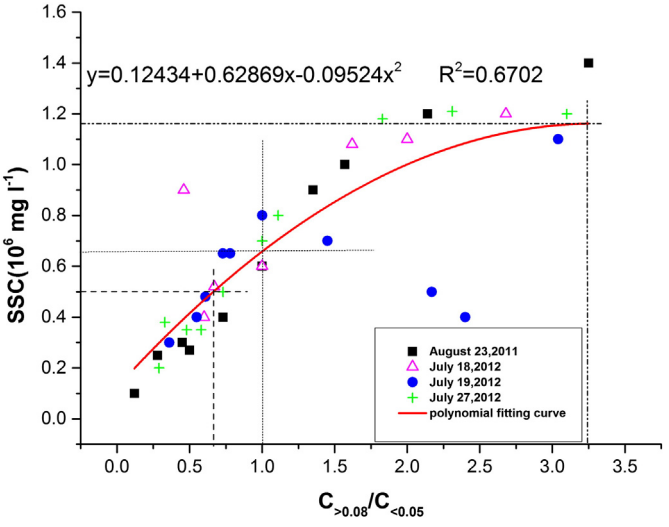

Fig. 10. The relationship between grain size combination and SSC in the four flood events.

The SDC experienced special fill-and-scour cycles over the study period due to seasonal alternate AFIs and channel erosion that substantially contributed to the total sediment yield in the Sudalaer watershed.

On 23 August 2011, a 35-min rainstorm in the upstream gully-dissected slopes led to 28.88×10^4 m^3 of flow discharge, which flushed downstream and eroded approximately 22.4×10^4 t of aeolian sands in the SDC to form an AHC flow (Ta et al., 2015) (Fig. 12a). After these flooding events, the SDC was filled with 8.66×10^4 t of aeolian sands between September 2011 and 17 July 2012, approximately all of which was contributed by W-, NWW-, NW-, NNW- and N- winds in March to May (spring season). After this input of aeolian sand, the SDC experienced three AHC flows in response to 30–45 min of heavy rainfall in July 2012. The high frequency of rainstorms was indeed a rare event, which led to the transport of approximately 28.9×10^4 t of aeolian sand out of the SDC (Ta et al., 2015) (Fig. 12b). Then, from August 2012 to July 2013, approximately 6.83×10^4 t of aeolian sand was transported to the desert channel, which when combined with the new aeolian sand supply, is likely to contribute to the fluvial sediment yield during subsequent flooding.

As shown in Fig. 12a, the total sediment yield during the AHC flows in the Sudalaer watershed on 23 August 2011 was 38.6×10^4 t, of which the coarse aeolian sediment yield contributed 58% of the total sediment yield (22.4×10^4 t). In addition, over the period of the three flooding events in July 2012, the erosion yield of the aeolian dunes (28.9×10^4 t) contributed 45% of the total sediment yield (64.16×10^4 t) (Fig. 12b). In total, the sediment yield ratio of aeolian erosion to fluvial erosion is 1:1.

Table 3
Annual channel scour in the SDC from 2011 to 2012.

Time (yr)	2011	2012
Channel scour (10^4 t)	22.4	28.9

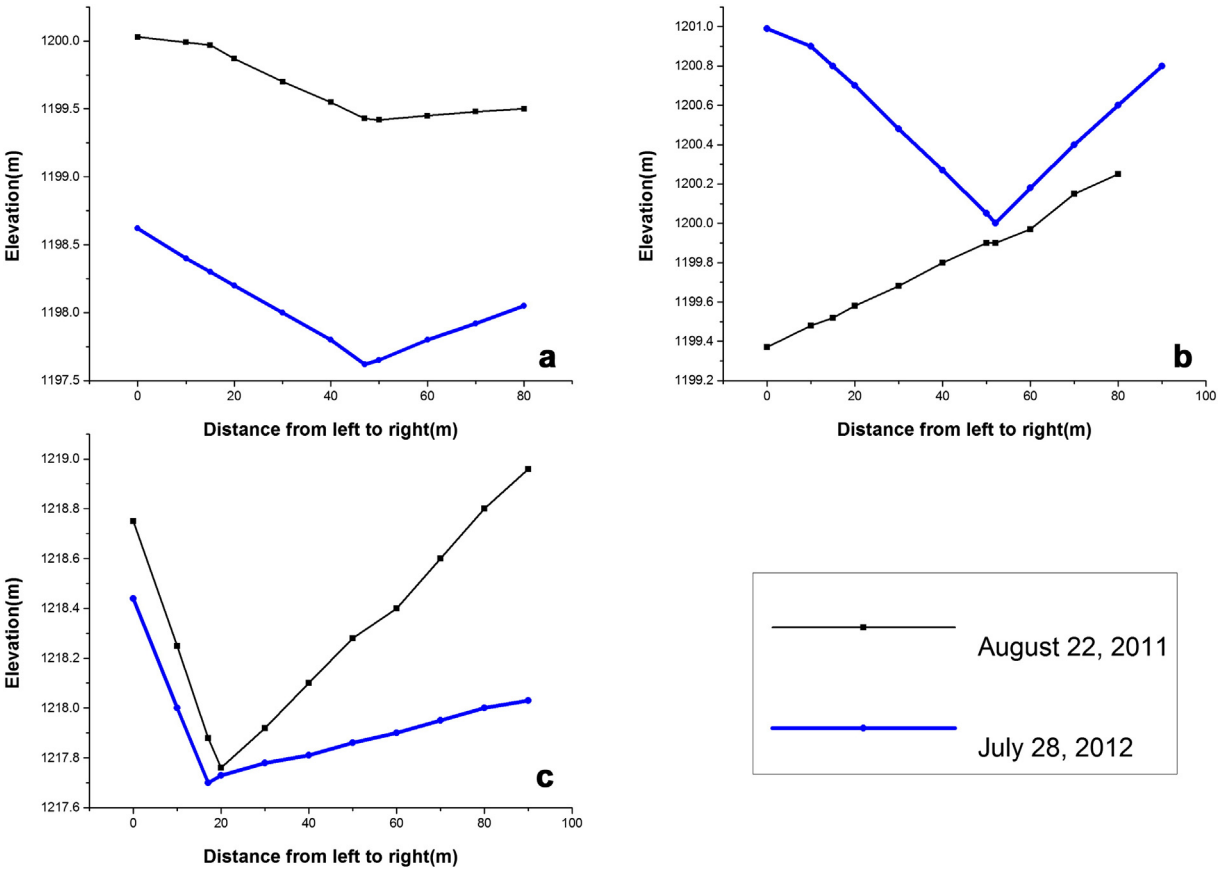

Fig. 11. The surveyed stream channel profiles with respect to fluvial erosion in the SDC: (a) No. 12; (b) No. 30; (c) No. 52.

These special fill-and-scour processes are not unique and have been observed in the Badonggou desert channel in the Ordos Plateau, which is one tributary of the Boersetai desert channel (T2, Fig. 1b). The sediment yield ratio of aeolian erosion to fluvial erosion was studied and was reported as 1.8:1 (Ma et al., 2013), which indicated and further supported the severe AFI in the arid desert watersheds in the upstream area of the Yellow River.

6. Conclusions

This study reports findings, from a more integrated perspective of aeolian-fluvial dynamics and describes the characteristics of AHC flows in response to severe AFI in the SDC in the upstream area of the Yellow River. A decreasing recirculation of airflow-induced wind speed was the main reason for channel filling during frequent sandstorm seasons in the aeolian dune area. The infrequent rainstorm-induced runoff with a threshold SSC γ_0 was critical for entraining more coarse aeolian sands available in the channel to form AHC flows and subsequent channel scour. AHC flows appear to be a natural consequence of seasonal alternate AFIs. Our analysis results indicate that there is an optimal grain size ratio of different grain size sediment contents in the flows, indicating the severity of the effects of aeolian and fluvial erosion on different earth surface materials. Following the OGI ($C_{>0.08}/C_{<0.05\ mm}$) we proposed for the first time, with respect to the SSC of AHC flows, the SSC $\gamma_0 = 500\ m^3\ s^{-1}$ was suggested as the threshold value for the occurrence of AHC flows in arid desert watersheds in the upstream area of the Yellow River. Because AHC flows always show very high rates of sediment transport and lead to deleterious

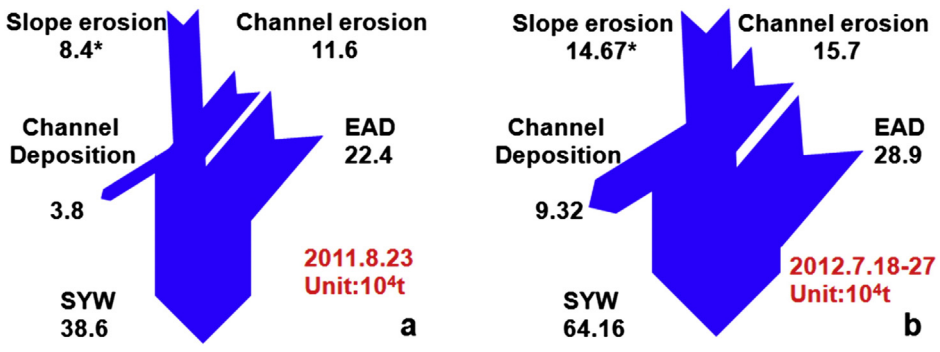

Fig. 12. Sediment budgets for the Sudalaer desert watershed and the contribution of the aeolian supply to the sediment yield: (a) 2011.8.23; (b) 2012.7.18-27; EAD: erosion of the aeolian dunes in the SDC; SYW: sediment yield from the Sudalaer desert watershed. *The values are derived from sediment budgets.

downstream effects on the river system and ecology, comprehensive governing of soil erosion in the upstream gully-dissected slopes is suggested as an essential and effective method for controlling AHC flows.

Acknowledgements

This work was supported by the National Basic Research Program of China (No. 2011CB403302), the Natural Science Foundation of China (No. 51269009 and No. 41171011) and the West Light Talents Foundation of CAS (29Y329971) "Transport Mechanism of coarse sediment in desert watershed in arid zones — a case of Ningxia-Inner Mongolia Reach of Yellow River" (2012). The authors acknowledge Dr. Gert Verstraeten and two anonymous reviewers for their reviews of the article, whose comments helped to greatly improve the article. The authors also thank Elsevier Language Editing Services (www.webshop.elsevier.com) for editorial help.

References

Anderson, S.P., Anderson, R.S., 1990. Debris-flow benches: dune-contact deposits record paleo-sand dune positions in north Panamint Valley, Inyo County, California. Geology 18, 524–527.
Bagnold, R.A., 1941. The Physics of Blown Sand and Desert Dunes. Methuen and Co., Ltd, London.
Belnap, J., Munson, S.M., Field, J.P., 2011. Aeolian and fluvial processes in dryland regions: the need for integrated studies. Ecohydrology 4, 615–622.
Breshears, D.D., Whicker, J.J., Johansen, M.P., Pinder, J.E., 2003. Wind and water erosion and transport in semi-arid shrubland, grassland and forest ecosystems: quantifying dominance of horizontal wind-driven transport. Earth Surf. Process. Landf. 28, 1189–1209.
Buckley, R., 1987. The effect of sparse vegetation on the transport of dune sand by wind. Nature 325, 426–428.
Bullard, J.E., Livingstone, I., 2002. Interactions between aeolian and fluvial systems in dryland environments. Area 34, 8–16.
Bullard, J.E., McTainsh, G.H., 2003. Aeolian-fluvial interactions in dryland environments: examples, concepts and Australia case study. Prog. Phys. Geogr. 27, 471–501.
Draut, A.E., 2012. Effects of river regulation on aeolian landscapes, Colorado River, southwestern USA. J. Geophys. Res. Earth Surf. 117, F02022–F02043.
Field, J.P., Breshears, D.D., Whicker, J.J., 2009. Toward a more holistic perspective of soil erosion: why aeolian research needs to explicitly consider fluvial processes and interactions. Aeolian Res. 1, 9–17.
Jackson, P., Hunt, J., 1975. Turbulent wind flow over a low hill. Q. J. R. Meteorol. Soc. 101, 929–955.
Jones, L.S., Blakey, R.C., 1997. Eolian-fluvial interaction in the Page Sandstone (Middle Jurassic) in south-central Utah, USA—a case study of erg-margin processes. Sediment. Geol. 109, 181–198.
Klein, M., 1984. Anti clockwise hysteresis in suspended sediment concentration during individual storms: Holbeck Catchment; Yorkshire, England. Catena 11, 251–257.
Lancaster, N., Baas, A., 1998. Influence of vegetation cover on sand transport by wind: field studies at Owens Lake, California. Earth Surf. Process. Landf. 23, 69–82.
Langford, R.P., 1989. Fluvial-aeolian interactions: part I, modern systems. Sedimentology 36, 1023–1035.
Liu, B., Coulthard, T.J., 2014. Mapping the interactions between rivers and sand dunes: implications for fluvial and aeolian geomorphology. Geomorphology 231, 246–257.
Ma, Y., Yang, P., Li, S., 2013. Dynamic process of aeolian-fluvial interaction erosion in the middle reaches of Baerdong river in ten-watershed, Inner Mongolia of China. J. Desert Res. 33, 10.
Marker, M.E., 1977. A long-return geomorphic event in the Namib Desert, South West Africa. Area 209–213.
Mason, J.P., Swinehart, J.B., Loope, D.B., 1997. Holocene history of lacustrine and marsh sediments in a dune-blocked drainage, southwestern Nebraska Sand Hills, USA. J. Paleolimnol. 17, 67–83.
Nanson, G., Chen, X., Price, D., 1995. Aeolian and fluvial evidence of changing climate and wind patterns during the past 100 ka in the western Simpson Desert, Australia. Palaeogeogr. Palaeoclimatol. Palaeoecol. 113, 87–102.
Onoe, N., Hashimoto, S., Sawada, H., 1985. Turbidity current with erosion and deposition. J. Hydraul. Eng. ASCE 111, 1473–1496.
Pantin, H.M., 1979. Interaction between velocity and effective density in turbidity flow: phase-plane analysis, with criteria for autosuspension. Mar. Geol. 31, 59–99.
Parker, G., Fukushima, Y., Pantin, H.M., 1986. Self-accelerating turbidity currents. J. Fluid Mech. 171, 145–181.
Sankey, J.B., Draut, A.E., 2014. Gully annealing by aeolian sediment: field and remote-sensing investigation of aeolian–hillslope–fluvial interactions, Colorado River corridor, Arizona, USA ☆. Geomorphology 220, 68–80.
Sauermann, G., Kroy, K., Herrmann, H.J., 2001. Continuum saltation model for sand dunes. Phys. Rev. E Stat. Nonlin. Soft Matter Phys. 64, 031305.
Smith, N.D., Smith, D.G., 1984. William River: an outstanding example of channel widening and braiding caused by bed-load addition. Geology 12, 78–82.
Ta, W., Xiao, H., Dong, Z., 2008. Long-term morphodynamic changes of a desert reach of the Yellow River following upstream large reservoirs' operation. Geomorphology 97, 249–259.
Ta, W., Wang, H., Jia, X., 2014. Aeolian process-induced hyper-concentrated flow in a desert watershed. J. Hydrol. 511, 220–228.
Ta, W., Wang, H., Jia, X., 2015. The contribution of aeolian processes to fluvial sediment yield from a desert watershed in the Ordos Plateau, China. Hydrol. Process. 29, 80–89.
Teller, J.T., Lancaster, N., 1986. Lacustrine sediments at Narabeb in the central Namib Desert, Namibia. Palaeogeogr. Palaeoclimatol. Palaeoecol. 56, 177–195.
Thomas, D.S., Stokes, S., Shaw, P.A., 1997. Holocene aeolian activity in the southwestern Kalahari Desert, southern Africa: significance and relationships to late-Pleistocene dune-building events. The Holocene 7, 273–281.
Tooth, S., 2000. Process, form and change in dryland rivers: a review of recent research. Earth Sci. Rev. 51, 67–107.
Tsoar, H., 1990. The ecological background, deterioration and reclamation of desert dune sand. Agric. Ecosyst. Environ. 33, 147–170.
Wasson, R.J., Nanninga, P.M., 1986. Estimating wind transport of sand on vegetated surfaces. Earth Surf. Process. Landf. 11, 505–514.
Winterwerp, J.C., Bakker, W.T., Mastbergen, D.R., Rossum, H.V., 1992. Hyperconcentrated sand-water mixture flows over erodible bed. J. Hydraul. Eng. 118, 1508–1525.
Wolfe, S.A., Nickling, W.G., 1993. The protective role of sparse vegetation in wind erosion. Prog. Phys. Geogr. 17, 50–68.
Xu, J., 2005a. Influence and significance of aeolian and fluvial interactions to grain size characteristics of suspended sediment of turbutaries of the Yellow River. Adv. Nat. Sci. 15, 7.
Xu, J., 2005b. Influence of aeolian and fluvial interactions to hyperconcentrated flows in the Yellow River basin. Sci. Sin. Terrae 35, 8.
Xu, J., 2013. Erosion and sediment yield of 10 small tributaries joining Inner Mongolia reach of upper Yellow River in relation with coupled wind-water processes and hyperconcentrated flows. J. Sediment. Res. 10.
Zhi, J.F., Shi, M.L., 2002. Cross-river sand dam formation response to confluence of extreme sediment loading flow into the Yellow River in July 21, 1989. In: Wang Gang, F.Z. (Ed.), Study on Change in Water and Sediment of the Yellow River. Yellow River Conservancy Press, Zhengzhou, pp. 460–471.